Effect of Hydration and Dimerization of the Formamidine Rearrangement

Kiet A. Nguyen,[†] Mark S. Gordon,*[,†] and Donald G. Truhlar[‡]

Contribution from the Department of Chemistry, North Dakota State University, Fargo, North Dakota 58105, and the Department of Chemistry and Supercomputer Institute, University of Minnesota, Minneapolis, Minnesota 55455. *Received August 10, 1990. Revised Manuscript Received October 29, 1990*

Abstract: Ab initio molecular orbital theory is used to predict the geometry of the transition state and the energy barrier for the double-proton transfer in formamidine dimer, using SCF/6-31G(d,p) and MP2/6-31G(d,p) wave functions, respectively. Intramolecular hydrogen transfer in the uncomplexed monomer (1) and double-proton transfer in the mixed dimer of formamidine and water (2) are also investigated at several levels of theory. All computational levels predict the barrier for the uncomplexed reaction (1) to be approximately twice that for the hydrated reaction (2). Isomerization by double-proton transfer in the dimer (3) is predicted to be the most favorable process. Indeed, for (3), the energy gained from the formation of the hydrogen-bonded complex is greater than the associated barrier for the double-proton transfer, thereby making this process very efficient.

I. Introduction

Amidine compounds are of interest because of their medical and biochemical importance.[1-5] They play a vital role in the biosynthesis of imidazole and purines and the catabolism of histidine. Biological activity studies have reported amidines to be antibiotic, antifungal, and anaesthetic.[2-4] Formamidine (methanimidamine $H_2N-CH=NH$), a small amidine which also has established biological activity,[6,7] has been the subject of both experimental and theoretical investigations and is of particular interest as a prototype for this class of compounds.

Since biological activity depends greatly on the molecular conformation, theoretical[1,8,9] studies of the *E* (trans) and *Z* (cis) configurations of formamidine have been performed. Calculations by Zielinski et al.,[1] using the 3-21G[10] basis set at the Hartree-Fock[11] (HF) level of theory, predict the *E* and *Z* configurations of formamidine to be separated only 0.6 kcal/mol (the *E* configuration is more stable) with an "in-plane isomerization" barrier of 23.4 kcal/mol. A stabilization energy of 2.94 kcal/mol[9] compared to the *Z* configuration is found for the *E* form of formamidine with the 4-31G[12] basis set at the same HF level of theory. A pseudopotential calculation[8] predicts the *E* configuration to lie 1.6 kcal/mol below the *Z* configuration on the potential energy surface. Experimentally, the relative energies of the two isomers and the interconversion rotational barrier have not been determined. However, experimental observations[13] of formamidine derivatives suggest the existence of two isomers. In additional experimental work, the kinetic isotope effects for double proton transfers have been studied in phenyl-substituted formamidines.[13d,e]

In addition to serving as a simple model for hydrogen shift reactions[14] and protonation and deprotonation[1] in bases of nucleic acids (e.g., adenine and cytosine), formamidine is a prime target for extensive theoretical investigations because it hydrogen bonds with itself and with water. The intramolecular hydrogen transfer in formamidine ([1,3] sigmatropic rearrangement, see Figure 1a) was first studied theoretically by Fukui and co-workers[15] using the 4-31G basis set at the HF level. A more recent theoretical investigation[14] of this system was performed at the HF level but with three larger basis sets [3-21G,[10] 6-31G,[16] and 6-31G(d,p)[17]], followed by CI calculations at the HF geometries. A very high barrier was reported for the intramolecular proton transfer at all levels of theory (52.6 kcal/mol at the highest level of theory[14]).

One mechanism for reducing the hydrogen-transfer barrier was considered by Fukui et al.,[18] who found that assistance by a water molecule (see Figure 1b) reduces the barrier by one-third compared to the intramolecular rearrangement at the same level of theory. A barrier of 21.6 kcal/mol was reported for this water-assisted formamidine rearrangement, using the 4-31G basis set at the HF level without correlation corrections. The reaction path was traced by using the minimum STO-3G[19] basis set at the HF level of theory, and the isotope effect[20] and tunneling probability[21] were also investigated. Another calculation[2] for the same mechanism, but with the 6-31G basis set, gave a 20.9 kcal/mol barrier.

The feasibility of double-proton transfer via the dimerization-assisted mechanism (Figure 1c) has been considered by Zielinski and Poirier.[22] Quantitive investigations, however, were performed by using the 3-21G basis set which is known to favor planar structures for nitrogen-containing compounds.[23,24] Minima

[†] North Dakota State University.
[‡] University of Minnesota.

(1) Zielinski, T. J.; Peterson, M. R.; Csizmadia, I. G.; Rein, R. *J. Comput. Chem.* **1982**, *3*, 62.
(2) Zielinski, T. J.; Poirier, R. A.; Peterson, M. R.; Csizmadia, I. G. *J. Comput. Chem.* **1983**, *4*, 419.
(3) Steinman, U.; Estler, C. J.; Pann, O. *Drug. Dev. Res.* **1986**, *7*, 153.
(4) Foussard-Blaupin, O.; Quevauviller, A. *Ann. Pharm. Fr.* **1982**, *40*, 231.
(5) Grant, R. J. In *The Chemistry of Amidines and Imidates*; Patai, S., Ed.; Wiley: New York, 1975; Chapter 6.
(6) Johnson, T. L.; Knowles, C. O. *Gen. Pharmacol.* **1983**, *14*, 591.
(7) Kaneda, M.; Oomura, Y.; Ishibashi, O.; Akaike, N. *Neurosci. Lett.* **1988**, *88*, 253.
(8) Kinasiewicz, W.; Les', A.; Wawer, I. *J. Mol. Struct. (THEOCHEM)* **1988**, *168*, 1.
(9) Radom, L.; Hehre, W. J.; Pople, J. A. *J. Am. Chem. Soc.* **1971**, *93*, 289.
(10) Binkley, J. S.; Pople, J. A.; Hehre, W. J. *J. Am. Chem. Soc.* **1980**, *102*, 939.
(11) Roothaan, C. C. J. *Rev. Mod. Phys.* **1951**, *23*, 69.
(12) Hehre, W. J.; Ditchfield, R.; Pople, J. A. *J. Chem. Phys.* **1971**, *54*, 724.
(13) (a) Hegathy, A. F.; Chandler, A. *Tetrahedron Lett.* **1980**, 885. (b) Filleux, M. L.; Naulet, N.; Doric, J. P.; Martin, G. J.; Pornet, J.; Miginiac, L. *Tetrahedron Lett.* **1974**, 1435. (c) Krajewski, J. W.; Urbanczyk-Lipkowska, Z.; Gluzinski, P.; Busko-Oszczapowicz, Z.; Bleidelis, J.; Kemme, A. *Pol. J. Chem.* **1981**, *55*, 1015. (d) Meschede, L.; Garritzen, D.; Limbach, H.-H. *Ber. Bunsenges. Phys. Chem.* **1988**, *92*, 469. (e) Limbach, H.-H.; Meschede, L.; Scherer, G. Z. *Naturforsch.* **1989**, *44a*, 459.
(14) Poirier, R. A.; Majlessi, D.; Zielinski, T. J. *J. Comput. Chem.* **1986**, *7*, 464.
(15) Yamashita, K.; Kaminoyama, M.; Yamabe, T.; Fukui, K. *Theor. Chim. Acta* **1981**, *60*, 303.
(16) Hehre, W. J.; Ditchfield, R.; Pople, J. A. *J. Chem. Phys.* **1972**, *56*, 2257.
(17) Hariharan, P. C.; Pople, J. A. *Theor. Chim. Acta* **1973**, *28*, 213.
(18) Yamabe, T.; Yamashita, K.; Kaminoyama, M.; Koizumi, M.; Tachibana, A.; Fukui, K. *J. Phys. Chem.* **1984**, *88*, 1459.
(19) (a) Hehre, W. J.; Stewart, R. F.; Pople, J. A. *J. Chem. Phys.* **1969**, *51*, 2657. (b) Hehre, W. J.; Ditchfield, R.; Stewart, R. F.; Pople, J. A. *J. Chem. Phys.* **1970**, *52*, 2769.
(20) Kato, S.; Fukui, K. *J. Am. Chem. Soc.* **1976**, *98*, 6395.
(21) (a) Marcus, R. A.; Coltrin, M. E. *J. Chem. Phys.* **1977**, *67*, 2609. (b) Marcus, R. A. *J. Chem. Phys.* **1979**, *83*, 204.
(22) Zielinski, T. J.; Poirier, R. A. *J. Comput. Chem.* **1984**, *5*, 466.

0002-7863/91/1513-1596$02.50/0

Table I. Barriers (kcal/mol) for the Intramolecular Proton Transfer

	6-31G(d,p)//SCF/6-31G		6-31G(d,p)//SCF/6-31G(d)				6-311G(d,p)//SCF/6-31G(d)		
	CISD	CISD-DQ	SCF	MP2	SAC2	MP4(SDTQ)	SCF	MP2	MP4(SDTQ)
$\Delta H_0^{\ddagger}$ [a]			56.6	42.8	39.7	43.9	57.5	42.6	43.4
$\Delta E^{\ddagger}$ [b]	54.5	52.6	60.6	46.9	43.8	48.0	61.6	47.7	47.5

[a] Corrected for vibrational zero point energy (ZPE). [b] Uncorrected for vibrational ZPE.

and transition states were not verified with force-field calculations in this investigation, and the importance of polarization functions and correlation corrections on the associated energetics was not considered. A recent theoretical investigation[25] on the dimerization-assisted double-proton transfer of formamidine was done with several basis sets at the HF level of theory. At the highest level of theory [SCF/6-31G(d)], double-proton-transfer transition states were not reported in this study. Furthermore, correlation corrections were not included at all of the important points on the potential energy surface.

Proton-transfer mechanisms of formamidine may be considered as basic models for proton transfer in bases of nucleic acid[2,26] and as a basic model for double-proton transfer.[26] They also provide a deeper understanding of hydrogen bonding, which is very important for biological activities of formamidine[6,7] as well as the qualitative picture of chemical bonding in the larger amidine families. Multiple-proton-transfer reactions are also implicated in the charge-relay mechanism of hydrolyses catalyzed by enzymes and other enzyme-catalyzed and water-catalyzed tautomerizations.[27]

In the present study, an investigation of the dimerization-assisted intermolecular hydrogen transfer in formamidine is carried out with a more extensive basis set than used previously and including electron correlation. Both concerted and nonconcerted mechanisms of the dimerization-assisted double-hydrogen transfer are examined. For comparison, calculations are also performed on the intermolecular water-assisted hydrogen transfer (Figure 1b) and the intramolecular hydrogen transfer (Figure 1a).

II. Computational Methods

Because the STO-3G basis set has only one contracted basis function for each component of a p orbital, one may expect it to underestimate the distance between the atoms in a hydrogen bond.[18] It is also well-known that basis sets without d functions at N favor planar structures.[23,24] Therefore, one needs a larger basis set, e.g., the 6-31G(d) basis, to obtain reasonable structures for the systems considered here.

All structures were optimized by using analytical energy gradients with the 6-31G(d) basis set[17,28] at the SCF level of theory[11] [SCF/6-31G(d)]. For the dimer-assisted double-proton-transfer mechanism, the 6-31G(d,p) basis set[17,28] was used to study the structural effects of polarization functions. Single-point correlation corrections were done with 6-31G(d,p) and the larger 6-311G(d,p)[29] basis sets with second-order (MP2) and fourth-order (MP4) many-body perturbation theory as formulated by Pople and co-workers[30] (only the valence electrons were correlated in all cases). All fourth-order calculations include the full set of single, double, triple, and quadruple (SDTQ) valence excitations. To obtain improved predictions for barrier heights, the MP-SAC extrapolation procedure[31] has been used with the 6-31G(d,p) basis set, without reoptimization of structures. The scale factor of 0.815 [the average of NH and OH values for the 6-31G(d,p) basis set] was used for these calculations. Minima and transition states were identified by diagonalizing the force constant matrices and verifying that they have zero and one negative eigenvalue, respectively.

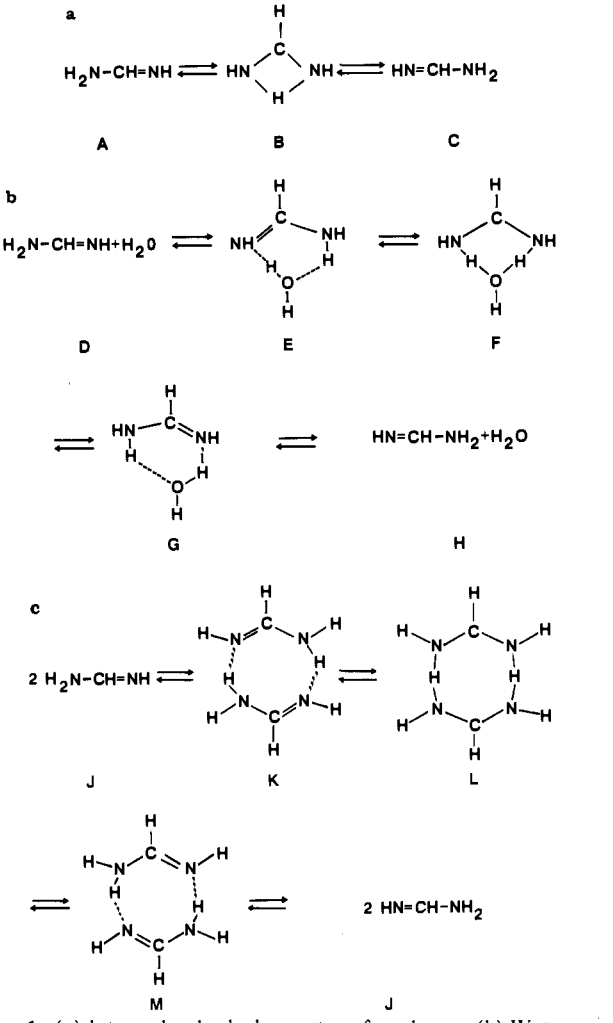

Figure 1. (a) Intramolecular hydrogen-transfer scheme. (b) Water-assisted intermolecular hydrogen-transfer scheme. (c) Dimerization-assisted intermolecular hydrogen-transfer scheme.

All ab initio electronic structure calculations were performed by using the GAMESS[32] and GAUSSIAN86[33] quantum chemistry programs. All SCF calculations are carried out in the restricted Hartree–Fock approximation. Except where indicated otherwise, zero-point vibrational energy corrections were included on the basis of the harmonic approximation. If $\Delta E^{\ddagger}$ is the electronic energy difference, including nuclear repulsions, between a transition state of a unimolecular process and the equilibrium structure of the reactant, the zero-point corrected barrier is

$$\Delta H_0^{\ddagger} = \Delta E^{\ddagger} + \tfrac{1}{2}\, hc[\sum_{m=1}^{3n-7} \nu_m^{\ddagger} - \sum_{m=1}^{3n-6} \nu_m^{R}]$$

where $\nu_m^{\ddagger}$ and ν_m^{R} are transition-state and reactant frequencies, respectively, and n is the number of atoms. Zero-point corrections for thermodynamic reaction enthalpies are carried out similarly except that both

(23) Body, R. G.; McClure, D. S.; Clementi, E. *J. Chem. Phys.* **1968**, *49*, 4916.
(24) Rauk, A.; Allen, L. C.; Clementi, E. *J. Chem. Phys.* **1970**, *52*, 4133.
(25) Svensson, P.; Bergman, N.-Å; Ahlberg, P. *J. Chem. Soc., Chem. Commun.* **1990**, 82.
(26) Scheiner, S.; Kern, C. W. *J. Am. Chem. Soc.* **1979**, *101*, 4081.
(27) Hibbert, F. *Adv. Phys. Org. Chem.* **1986**, *22*, 113.
(28) Francl, M. M.; Pietro, W. J.; Hehre, W. J.; Binkley, J. S.; Gordon, M. S.; DeFrees, J. D.; Pople, J. A. *J. Chem. Phys.* **1982**, *77*, 3654.
(29) Krishnan, R.; Binkley, J. S.; Seeger, R.; Pople, J. A. *J. Chem. Phys.* **1980**, *72*, 650.
(30) (a) Møller, Plesset, M. S. *Phys. Rev.* **1934**, *46*, 618. (b) Pople, J. A.; Binkley, J. S.; Seeger, R. *Int. J. Quantum Chem. Symp.* **1976**, *10*, 1. (c) Pople, J. A.; Seeger, R.; Krishnan, R. *Int. J. Quantum Chem. Symp.* **1977**, *11*, 149. (d) Krishnan, R.; Pople, J. A. *Int. J. Quantum Chem.* **1978**, *14*, 91. (e) Krishnan, R.; Frisch, M. J.; Pople, J. A. *J. Chem. Phys.* **1980**, *72*, 4244.
(31) Gordon, M. S.; Truhlar, D. G. *J. Am. Chem. Soc.* **1986**, *108*, 5412.
(32) (a) Dupuis, M.; Spangler, D.; Wendoloski, J. J. *National Resource for Computation in Chemistry Software Catalog*; University of California: Berkeley, 1980; Prog. QG01. (b) Schmidt, M. W.; Boatz, J. A.; Baldridge, K. K.; Koseki, S.; Gordon, M. S.; Elbert, S. T.; Lam, B. *QCPE Bull.* **1978**, *7*, 115.
(33) Frisch, M. J.; Binkley, J. S.; Schlegel, H. B.; Ragahvachari, K.; Melius, C. F.; Kahn, L. R.; DeFrees, D. J.; Seeger, R.; Whiteside, R. A.; Rohlfing, C. M.; Fox, D. J.; Fleuder, E. M.; Pople, J. A. GAUSSIAN 86; Carnegie-Mellon Quantum Chemistry Publishing Unit: Pittsburgh, PA, 1984.

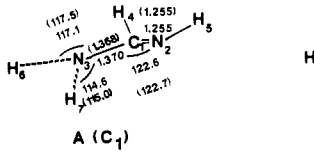

Figure 2. RHF/6-32G(d) structures, bond distances (R), and bond angles (A, ω-dihedral) with RHF/6-31G(d,p) bond distances and bond angles in parentheses. Bond lengths are in angstroms; angles are in degrees. (A) Formamidine: $R(1,4)$ = 1.084 (1.085), $R(2,5)$ = 1.002 (1.001), $R(3,6)$ = 0.996 (0.994), $R(3,7)$ = 0.998 (0.996); $A(4,1,2)$ = 124.4 (124.4), $A(5,2,1)$ = 111.1 (111.1); $\omega(4,1,2,3)$ = 177.5 (177.7), $\omega(5,2,1,3)$ = 183.8 (183.6), $\omega(6,3,1,2)$ = −152.0 (−153.6), $\omega(7,3,1,2)$ = −14.0 (−12.9). (B) Intramolecular proton-transfer transition state; $R(1,2)$ = 1.079, $R(5,2)$ = 1.632, $R(6,3)$ = 0.998; ω = 157.9.

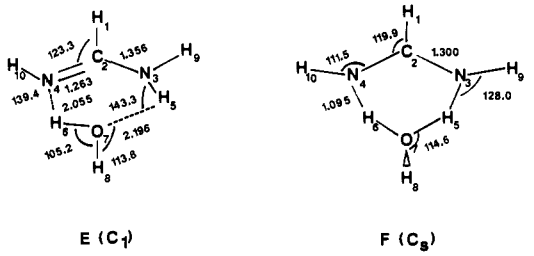

Figure 3. RHF/6-31G(d) structures. Bond lengths (R) are in angstroms; angles (A, ω-dihedral) are in degrees. (E) Formamidine–water complex: $R(1,2)$ = 1.083, $R(5,3)$ = 1.001, $R(7,6)$ = 0.958, $R(9,3)$ = 0.994, $R(8,7)$ = 0.974, $R(10,4)$ = 1.001; $A(1,2,3)$ = 113.5, $A(5,3,2)$ = 116.6, $A(5,3,9)$ = 116.5, $A(6,4,2)$ = 108.2; $\omega(4,2,3,1)$ = 178.0, $\omega(5,3,2,1)$ = 190.9, $\omega(6,3,2,1)$ = 170.6, $\omega(7,5,3,2)$ = −9.1, $\omega(9,3,5,7)$ = 203.6, $\omega(10,3,6,7)$ = 180.7. (F) Water-assisted double-proton-transfer transition state: $R(2,1)$ = 1.078, $R(2,7)$ = 2.860, $R(3,9)$ = 0.994, $R(7,8)$ = 0.948; ω-(4,2,3,9) = 179.8, $\omega(10,4,2,1)$ = 181.9, $\omega(10,4,6,7)$ = 186.6.

sums, over product modes and over reactant modes, have $3n - 6$ terms.

III. Results and Discussion

A. Intramolecular Proton Transfer. The transition-state structure obtained by Fukui et al.,[15] at the SCF/4-31G level, has C_{2v} symmetry, but the C_{2v} stationary point has two imaginary frequencies at the SCF/6-31G(d) level. Only one true nonplanar transition state is found, and it has C_s symmetry and a large imaginary frequency (2440i cm^{-1}). This frequency indicates that the potential energy barrier is very narrow. The fully optimized transition state and the minimum-energy formamidine structures are shown in Figure 2. The calculated MP4/6-311G(d,p)//SCF/6-31G(d) barrier to intramolecular hydrogen transfer is 43.4 kcal/mol (see Table I; "//" means "at the geometry of"), which is much lower than the SCF/4-31G value (59.1 kcal/mol) reported earlier.[15] A significant difference is also found between the MP4(SDTQ)/6-31G(d,p)//SCF/6-31G(d) and CISD/6-31G-(d,p)//SCF/6-31G calculations,[14] as shown in Table I. Note also that at the MP4 level there is little difference between the barriers predicted with the 6-31G(d,p) and 6-311G(d,p) basis sets. These results illustrate that both polarization functions and correlation corrections are important for the description of the intramolecular hydrogen transfer, but expansion of the valence basis from double zeta to triple zeta is less important.

Finally, the intramolecular proton-transfer barriers calculated at the MP2/6-31G(d,p) level of theory were scaled by the MP2-SAC2 method (SAC2), to estimate the remaining correlation energy contribution to the MP2 barrier energy. SAC2 predicts a barrier of 39.7 kcal/mol (see Table I) for the [1,3] sigmatropic rearrangement in formamidine.

B. Intermolecular Double-Proton Transfer in the Formamidine–Water System. The SCF/6-31G(d) structures of the stationary points E and F (Figure 1b) on the potential energy surface are shown in Figure 3. As noted earlier,[2,18] the eqilibrium structure E is considered the starting point for this intermolecular hydrogen-transfer reaction. The hydrogen-bonded structure E is an intermediate on the reaction path in the reaction scheme shown in Figure 1b.

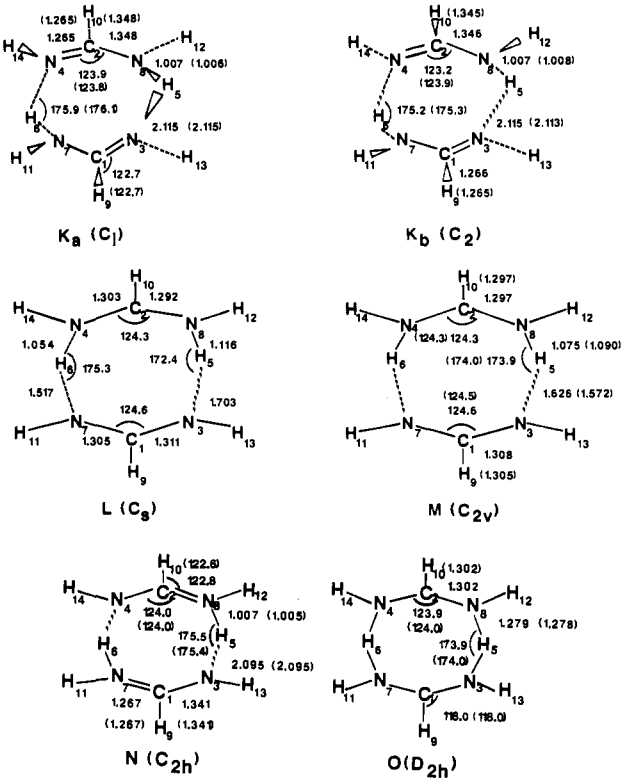

Figure 4. RHF/6-31G(d) structures, bond distances, and bond angles with RHF/6-31G(d,p) bond distances and bond angles in parentheses. Bond lengths (R) are in angstroms; angles (A, ω-dihedral) are in degrees. (K) formamidine dimers. (K_a): $R(9,1)$ = 1.085 (1.085), $R(11,7)$ = 0.993 (0.992), $R(13,3)$ = 1.002 (1.000); $A(10,2,4)$ = 122.7 (122.7), $A(14,4,2)$ = 110.9 (110.9), $A(5,3,1)$ = 120.0 (120.0), $A(6,7,1)$ = 119.0 (119.0), $A(11,7,1)$ = 118.3 (118.2); $\omega(5,3,1,7)$ = 12.4 (12.2), $\omega(10,2,4,8)$ = −178.1 (−178.3), $\omega(11,7,1,3)$ = −164.0 (−164.2), $\omega(14,4,2,8)$ = 177.4 (177.7). (K_b): $R(9,1)$ = 1.084 (1.086), $R(11,7)$ = 0.993 (0.991), R-(13,3) = 1.002 (1.001); $A(10,2,4)$ = 122.8 (122.7), $A(14,4,2)$ = 110.9 (110.9), $A(5,3,1)$ = 120.0 (120.0), $A(6,7,1)$ = 119.8 (119.7), $A(11,7,1)$ = 118.8 (118.8), $\omega(5,3,1,7)$ = −2.8 (−3.0), $\omega(10,2,4,8)$ = 178.4 (178.6), $\omega(11,7,1,3)$ = −167.8 (−168.3), $\omega(14,4,2,8)$ = −178.0 (−178.2). (L) Nonconcerted dimer-assisted double-proton-transfer transition state: $R(9,1)$ = 1.091, $R(10,2)$ = 1.079, $R(11,7)$ = 0.999, $R(12,8)$ = 0.994, $R(13,3)$ = 1.000, $R(14,4)$ = 0.996; $A(2,4,6)$ = 122.1, $A(2,8,5)$ = 121.3, $A(1,7,6)$ = 121.1, $A(1,3,5)$ = 118.9, $A(9,1,3)$ = 117.2, $A(10,2,4)$ = 117.2, $A(11,7,5)$ = 118.8, $A(12,8,2)$ = 117.6, $A(13,3,1)$ = 112.2, A-(11,7,1) = 111.3. (M) Concerted dimer-assisted double-proton-transfer transition state: $R(10,2)$ = 1.008 (1.008), $R(9,1)$ = 1.092 (1.092), $R(12,8)$ = 0.995 (0.993), $R(13,3)$ = 1.000 (0.999); $A(10,2,8)$ = 117.8 (117.8), $A(12,8,2)$ = 118.4 (117.7), $A(9,1,3)$ = 117.7 (117.8), $A(13,3,1)$ = 111.6 (111.7), $A(2,8,5)$ = 121.7 (121.5), $A(5,3,1)$ = 119.9 (120.0). (N,O) Stationary points with two imaginary frequencies. (N): $R(10,2)$ = 1.084 (1.086), $R(12,8)$ = 1.001 (1.001), $R(13,3)$ = 0.991 (0.990); $A(12,8,2)$ = 110.8 (110.8), $A(13,3,1)$ = 120.0 (120.0), $A(2,8,5)$ = 119.4 (119.8), $A(5,3,1)$ = 121.3 (120.8). (O): $R(10,2)$ = 1.086 (1.084), $R(12,8)$ = 0.996 (997); $A(12,8,2)$ = 123.9 (124.2), $A(5,8,2)$ = 121.1 (121.0).

Energetically, the overall MP4/6-311G(d,p) energy barrier (the difference between the reactant D and the transition-state F in the reaction scheme of Figure 1b) for the intermolecular water-assisted proton transfer is 6.8 kcal/mol, as shown in Table II. This is significantly lower than the value, 21.6 kcal/mol, previously reported[18] by Fukui and co-workers. The barrier is lowered almost to zero (0.7 kcal/mol) by extrapolating with SAC2/6-31G(d,p). As noted for the intramolecular hydrogen transfer, both polarization functions and correlation corrections play a major role in determining the potential energy barrier for this process (see Table II). The results in Table II illustrate that the assistance of a water molecule lowers the barrier for the hydrogen transfer by 36.6 kcal/mol, relative to the intramolecular transfer, at the MP4/6-311G(d,p) level of theory, including zero-point corrections, and by a similar amount at the SAC2/6-31G(d,p) level. The net

Table II

(A) Zero-Point Corrected Energy Differences (kcal/mol) and Barriers for the Water-Assisted Proton Transfer

	6-311G(d,p)//SCF/6-31G(d)			6-31G(d,p)//SCF/6-31G(d)			
reaction	SCF	MP2	MP4(SDTQ)	SCF	MP2	SAC2	MP4(SDTQ)
D → E[a]	−12.4	−12.8	−15.1	−12.7	−15.8		−15.4
E → F	29.4	20.9	21.9	28.6	19.3	17.2	20.7
D → F	17.0	8.1	6.8	15.9	3.5	0.7	5.3

(B) Uncorrected Zero-Point Energy Differences (kcal/mol) and Barriers for the Intramolecular Proton Transfer

	6-311G(d,p)//SCF/6-31G(d)			6-31G(d,p)//SCF/6-31G(d)			
reaction	SCF	MP2	MP4(SDTQ)	SCF	MP2	SAC2	MP4(SDTQ)
D → E[a]	−9.7	−12.8	−12.4	−10.0	−13.1		−12.7
E → F	32.1	23.6	24.6	31.4	22.1	20.0	23.5
D → F	22.4	10.8	12.2	11.4	9.0	8.5	10.8

[a] Thermodynamic energy difference; others are barriers.

Table III

(A) Barriers (kcal/mol) for the Intermolecular Dimerization-Assisted Proton Transfer

	SCF/6-31G(d)// SCF/6-31G(d)		6-31G(d,p)//SCF/6-31G(d)					
			SCF		MP2		SAC2	
	$\Delta E^{\ddagger}$	$\Delta H_0^{\ddagger}$	$\Delta E^{\ddagger}$	$\Delta H_0^{\ddagger}$	$\Delta E^{\ddagger}$	$\Delta H_0^{\ddagger}$	$\Delta E^{\ddagger}$	$\Delta H_0^{\ddagger}$
J → 0 (D_{2h})	18.4	13.8	14.7	10.1	−1.4	−6.0	−5.1	−9.7
K_a → L (C_s)	25.4	23.0	23.8	21.4	16.9	14.5	15.3	12.9
K_b → L (C_s)	25.3	23.1	23.7	21.5	16.8	14.6	15.2	13.0
K_a → 0 (D_{2h})	29.6	23.4	26.2	20.0	14.0	7.8	11.2	5.0

(B) Zero-Point Corrected Energy Differences (kcal/mol) for the Intermolecular Dimerization Process

	SCF/6-31G(d)//SCF/6-31G(d)		MP2/6-31G(d,p)//SCF/6-31G(d)	
	ΔE	ΔH_0	ΔE	ΔH_0
J → K_a (C_i)	−11.2	−9.6	−15.4	−13.8
J → K_b (C_2)	−11.1	−9.6	−15.2	−13.8
J → M (C_{2v})	14.2	14.2	2.1	2.1
J → N (C_{2h})	−11.0	−10.1	−15.2	−14.3

(C) Barriers (kcal/mol) for the Intermolecular Dimerization-Assisted Proton Transfer

	SCF/6-31G(d,p)// SCF/6-31G(d,p)		6-31G(d,p)//SCF/6-31G(d,p)			
			MP2		SAC2	
	$\Delta E^{\ddagger}$	$\Delta H_0^{\ddagger}$	$\Delta E^{\ddagger}$	$\Delta H_0^{\ddagger}$	$\Delta E^{\ddagger}$	$\Delta H_0^{\ddagger}$
J → 0 (D_{2h})	14.7	10.5	−1.6	−5.8	−5.3	−9.5
J → M (C_{2v})	12.4	11.7	0.9	0.2	−1.7	−2.4
K_a → M (C_{2v})	23.8	21.6	16.3	14.1	14.6	12.4
K_b → M (C_{2v})	23.8	21.7	16.2	14.1	14.5	12.4
K_a → 0 (D_{2h})	26.1	20.4	13.8	8.1	11.0	5.3
K_b → 0 (D_{2h})	26.1	20.5	13.7	8.1	11.0	5.3

(D) Energy Differences (kcal/mol) for the Intermolecular Dimerization Process

	SCF/6-31G(d,p)//SCF/6-31G(d,p)		MP2/6-31G(d,p)//SCF/6-31G(d,p)	
	ΔE	ΔH_0	ΔE	ΔH_0
J → K_a (C_i)	−11.4	−9.9	−15.4	−13.9
J → K_b (C_2)	−11.4	−10.0	−15.3	−13.9
J → N (C_{2h})	−11.4	−10.3	−15.3	−14.2

energy cost for the overall process (energy lowering due to hydrogen bond formation plus the barrier for water-assisted proton transfer) is 6.8 kcal/mol at the MP4(SDTQ)/6-311G(d,p) level of theory and 0.7 kcal/mol when SAC2/6-31G(d,p) is used.

C. **Intermolecular Dimer-Assisted Double-Hydrogen Transfer.** Six stationary points were located on the dimer potential energy surface at several levels of theory. The following discussion will be focused mainly on the minima and transition-state structures. In view of the small differences seen in Tables I and II between relative energies predicted by the 6-31G(d,p) and 6-311G(d,p) basis sets and at the MP2 and MP4 levels of theory, the dimer energetics have been predicted at the MP2/6-31G(d,p)//SCF/6-31G(d) and MP2/6-31G(d,p)//SCF/6-31G(d,p) levels of theory.

The dimerization of formamidine (reaction J → K in Figure 1c) leads to two stable structures with C_i and C_2 symmetry. Both of these are verified minima on the SCF/6-31G(d) and SCF/6-31G(d,p) potential energy surfaces. These structures, K_a and K_b (shown in Figure 4), are presumably intermediates in the dimerization-assisted double-proton transfer (Figure 1c). The structures and energetics for these two species are virtually identical (see Table III and Figure 4). Dimerization enthalpies for both the C_i and C_2 structures are exothermic by 13.8 kcal/mol at the MP2/6-31G(d,p)//SCF/6-31G(d) level of theory. This may be compared with a stabilization energy of 15.8 kcal/mol for the formamidine–water dimer at the same level of theory. (Both values include zero-point corrections.) Insignificant changes of both structures and relative energies of the two C_i and C_2 dimers are observed upon going from the 6-31G(d) to the 6-31G(d,p) basis set.

Structure N with C_{2h} symmetry is fully optimized to a verified minimum on the potential energy surface by using both STO-3G and 3-21G basis sets. However, two imaginary frequencies, with the displacement vectors of the normal modes corresponding to

out-of-plane bending motions, are obtained with the larger 6-31G(d) and 6-31G(d,p) basis set for this planar structure.

The concerted double-hydrogen transfer transition state with D_{2h} symmetry, structure O in Figure 4, is not a true transition state on either the 6-31G(d) or 6-31G(d,p) potential energy surface. This structure has two imaginary frequencies in both basis sets. One of these frequencies corresponds to the concerted double-proton transfer, where two hydrogens move simultaneously. Following the other mode leads to the structure M, which is a minimum with C_{2v} symmetry on the 6-31G(d) potential energy surface. However, one imaginary frequency is obtained for M with the 6-31G(d,p) basis. This structure (M) lies 4.2 and 2.3 kcal/mol below O (without zero-point correction) at the SCF/6-31G(d) and SCF/6-31G(d,p) levels, respectively. The order, however, is reversed at the MP2 level of theory. MP2/6-31G(d,p)//SCF/6-31G(d) and MP2/6-31G(d,p)//SCF/6-31G(d,p) predict O to lie 3.5 and 2.5 kcal/mol below M, respectively (without zero-point correction).

The nonsymmetric transition state L with C_s symmetry has one imaginary frequency ($328i$ cm^{-1}). This is apparently the lowest energy saddle point on the SCF/6-31G(d) potential energy surface for the nonconcerted double-proton transfer in the dimer. However, a SCF/6-31G(d,p) transition-state search starting at the SCF/6-31G(d) structure L leads to structure O with C_{2v} symmetry. Energetically, the MP2/6-31G(d,p)//SCF/6-31G(d) calculation predicts structure O to be the one with the lowest overall barrier (see Table IIIC) for the dimerization-assisted double-proton transfer. This process is exothermic by 5.3 kcal/mol (without zero-point corrections) as predicted by the MP-SAC2/6-31G(d,p) method. The net energy cost for the dimer-assisted proton transfer (energy lowering due to dimer formation plus the barrier to proton transfer) is −5.3 kcal/mol.

IV. Summary and Conclusions

The present study has employed high levels of electronic structure theory to compare the [1,3] N-to-N sigmatropic rearrangement of formamidine for three mechanisms: (1) intramolecular proton transfer, (2) water-assisted double-proton transfer, and (3) dimerization-assisted double-proton transfer. All computational levels predict the barrier for (1) to be approximately twice that for (2). Energetically, the dimerization-assisted double-proton transfer appears to be the most favorable process with an enthalpy of activation of −5.8 kcal/mol followed by the water-assisted (3.5 kcal/mol) and the intramolecular (42.8 kcal/mol) processes, as predicted by MP2/6-31G(d,p). In all cases, MP-SAC2 calculations reduce the barriers, by 3–4 kcal/mol. The double-proton transfer is found to be a rather low energy process, due in large part to the energy gained by the formation of hydrogen bonds.

The water-assisted and dimerization-assisted processes are extremely sensitive to the basis sets used. To obtain reliable energetics, correlation corrections must be and were incorporated in the calculations. Polarization functions on hydrogen are also essential to locate the transition state of the dimer double-proton transfer.

We plan in future work to continue the present study by calculating rate coefficients using the present structural studies as a starting point.

Acknowledgment. This work was supported in part by the National Science Foundation (Grants CHE86-17063, CHE89-11911, and CHE89-22048) and by the Donors of the Petroleum Research Fund, administered by the American Chemical Society. These calculations were performed in part on the CRAY 1 at the Minnesota Supercomputer Institute and in part on the North Dakota State University IBM 3090 (aided by a joint study agreement with IBM) and on the NDSU Quantum Chemistry VAX 8530 (funded by a grant from the Air Force Office of Scientific Research).

Registry No. Formamidine, 463-52-5.

Crown Thioether Chemistry. The Rhodium Complexes of 1,4,7-Trithiacyclononane (9S3) and 1,5,9-Trithiacyclododecane (12S3) and the Conformational Factors That Stabilize Monomeric Rh(II) Ions

Stephen R. Cooper,* Simon C. Rawle, Rahmi Yagbasan, and David J. Watkin

Contribution from the Inorganic Chemistry Laboratory and Chemical Crystallography Laboratory, University of Oxford, Oxford OX1 3QR, England. *Received July 18, 1990*

Abstract: Reaction of the trithia ligands 9S3 (1,4,7-trithiacyclononane), 10S3 (1,4,7-trithiacyclodecane), 12S3 (1,5,9-trithiacyclododecane), and ttn (2,5,8-trithianonane) with rhodium(III) triflate in methanol yields the homoleptic thioether complexes $[Rh(L)_2]^{3+}$ (L = 9S3, 10S3, 12S3, and ttn). Average Rh–S distances in these cations increase from 2.34 Å in the 9S3 complex to 2.36 Å in the 12S3 analogue. Cyclic voltammetry in $MeNO_2$ shows that $[Rh(9S3)_2]^{3+}$ undergoes *two one-electron reductions*. The first of these corresponds to a discrete mononuclear Rh(II) complex that has been characterized by EPR as well as electrochemical methods. The 10S3 analogue, $[Rh(10S3)_2]^{3+}$, behaves similarly. In the 12S3 analogue the quasi-reversible Rh(III/II) couple contrasts with the irreversibility of the Rh(II/I) process. In continuation of this trend, the acyclic complex $[Rh(ttn)_2]^{3+}$ shows no reversible electrochemistry. The conformational properties of the macrocyclic ligand play a crucial role in stabilizing $[Rh(L)_2]^{2+}$ complexes, as shown by their increasing stability to disproportionation in the order L = 9S3 > 10S3 > 12S3 ≫ ttn. Crystal data: $[Rh(9S3)_2](CF_3SO_3)_3$, $RhC_{15}H_{24}S_9F_9O_9$, fw = 910.83, monoclinic, space group $C2/c$ (no. 15), a = 18.638 (6) Å, b = 10.643 (3) Å, c = 16.075 (2) Å, β = 105.93 (2)°, Z = 4; $[Rh(12S3)_2](BF_4)_3$, $RhC_{18}H_{36}S_6B_3F_{12}$, fw = 808.2, monoclinic, space group $P2_1/c$ (no. 14), a = 17.673 (5) Å, b = 10.874 (4) Å, c = 17.164 (3) Å, β = 110.85 (1)°, Z = 4.

Introduction

Complexes of crown thioethers such as 1,4,7-trithiacyclononane (9S3)[1] often display remarkable features (e.g., unusual stability or spin or oxidation states) that differ qualitatively from apparently analogous complexes of other thioethers.[2-4] Examples include complexes containing low-spin six-coordinate Co(II),[5] Pd(III),[6]

* To whom correspondence should be addressed.

(1) Abbreviations used: 9S3, 1,4,7-trithiacyclononane; 10S3, 1,4,8-trithiacyclodecane; 12S3, 1,5,9-trithiacyclododecane; 14S4, 1,4,8,11-tetrathiacyclotetradecane; ttn, 2,5,8-trithianonane.

0002-7863/91/1513-1600$02.50/0